Eur. Phys. J. D **46**, 453–461 (2008)
DOI: 10.1140/epjd/e2008-00004-8

THE EUROPEAN PHYSICAL JOURNAL D

Independent particle model of spontaneous symmetry breaking in planar π-electron systems

G. Thiamová[1,2,a] and J. Paldus[1,b]

[1] Department of Applied Mathematics, University of Waterloo, Waterloo, Ontario N2L 3G1, Canada
[2] Nuclear Physics Institute, Czech Academy of Sciences, Prague-Řež, Czech Republic

Received 22 August 2007
Published online 11 January 2008 –

Abstract. The singlet stability of symmetry adapted (SA), restricted Hartree-Fock (RHF) solutions, and the implied symmetry breaking for several planar, π-electron systems, is investigated using the semiempirical Pariser-Parr-Pople Hamiltonian in the whole range of the coupling constant. We focus here on highly symmetric cyclic polyenes $C_{10}H_{10}$ and $C_{14}H_{14}$ and their various distorted analogues of lower symmetry, in particular on the perimeter models of naphthalene and anthracene (p-naphthalene and p-anthracene) modeling the so-called [n]-annulenes. Relying on earlier results for general systems with conjugated double-bonds, we explore the character and properties of both the SA and broken-symmetry (BS) RHF solutions for these systems and relate their behavior to those of highly symmetric cyclic polyenes and corresponding polyacenes. In this way we are able to provide a better understanding of the spontaneous symmetry breaking in these systems at the Hartree-Fock level of approximation.

PACS. 31.15.bu Semi-empirical and empirical calculations (differential overlap, Hückel, PPP methods)

1 Introduction

The Thouless stability conditions [1] for the solutions of the Hartree-Fock (HF) equations in the case of closed-shell atomic and molecular systems have been studied in reference [2]. For a spin-independent electronic Hamiltonian these stability conditions can be significantly simplified and the two types of eventual instabilities can be classified as the *singlet* and *nonsinglet* (or *triplet*) ones. This can be understood if we realize that a nonsinglet instability does not impose double-occupancy of spatial orbitals, thus allowing the use of different orbitals for different spins [DODS or unrestricted HF (UHF) approximation]. In such a way a substantial decrease in the variational energy may be achieved as a result of spin-polarization effects. Consequently, this type of instability is always found in open-shell systems [3]. In contrast, the singlet instability is generally related to the breaking of spatial symmetry, represented by the invariance point group of the fixed nuclear framework characterizing the Born-Oppenheimer electronic Hamiltonian.

Taking into account only the one-electron component of the electronic Hamiltonian (Hückel approximation), the single (antisymmetrized) product wave function will be automatically both spin and space symmetry adapted (SA), and any admixture of virtual orbitals to any of the occupied ones will only increase the energy of the system [4]. However, when the interelectronic interaction, i.e. the two-body part of the Hamiltonian, is turned on, the SA solution may no longer represent the absolute minimum or, in fact, even a local minimum in the variational space considered. Thus, the interplay between the one and two-body components of the Hamiltonian determines the stability of the SA solution: the more dominant the one-body component becomes, the less likely the SA solution will be unstable. The presence of a singlet instability of a SA solution then implies the existence of a broken symmetry (BS) pure singlet solution that has a lower energy than the SA one. We recall that this phenomenon represents an example of the so-called "symmetry dilemma" of Löwdin [5].

The HF energy and equations can be obtained as a solution of HF equations, which represent the necessary and sufficient conditions for the vanishing of the first variation $\delta^{(1)}E(\Phi)$ of the mean energy functional

$$E(\Phi) = \frac{\langle\Phi|H|\Phi\rangle}{\langle\Phi|\Phi\rangle}, \tag{1}$$

in the variational space spanned by the determinantal wave functions $|\Phi\rangle$

$$\Phi = \frac{1}{\sqrt{N!}} \det||\phi_1, \phi_2, ..., \phi_N||, \tag{2}$$

where ϕ_i, $(i = 1, \cdots, N)$ designate orthonormal molecular spin-orbitals.

[a] e-mail: thiamova@scienide.uwaterloo.ca
[b] Also at: Department of Chemistry and (GWC)^2 - Waterloo Campus, University of Waterloo, Waterloo, Ontario N2L 3G1, Canada.

In general, the mean energy hypersurface $E(\Phi)$, equation (1), defined on a manifold (2), may posses many stationary points characterized by the vanishing first variation $\delta^{(1)}E(\Phi)$, which may be associated with various HF solutions. Of course, the vanishing of the first variation $\delta^{(1)}E(\Phi)$ only guarantees that the solution corresponds to some stationary point on the energy hypersurface and, in fact, need not represent even a minimum (local or global).

The number and the character of HF solutions depends on the variational manifold to which the trial wave function belongs. Typically, this manifold consists of wave functions possessing the (spin and space) symmetry implied by the symmetry of the Hamiltonian. The resulting solutions are then referred to as the SA restricted HF (RHF) solutions. Of course, the imposition of such symmetry constraints on the variational problem for $E(\Phi)$, equation (1), can only raise the variational energy. By allowing broken symmetry (BS) solutions, the upper bound to the energy can be improved. This fact is the essence of the above mentioned symmetry dilemma of Löwdin.

The concept of a stability of HF solutions was first introduced by Thouless [1], who considered the second variation $\delta^{(2)}E(\Phi)$ of the mean energy functional (1), and formulated general stability conditions. Thus, a HF solution corresponds to a (local or global) minimum if $\delta^{(2)}E(\Phi) > 0$. Since $\delta^{(2)}E(\Phi)$ can be expressed as a quadratic form in terms of suitable variational parameters, the stability conditions may be characterized by an associated eigenvalue problem. A stable solution is then obtained if all the eigenvalues of the stability problem are positive, while one or more negative eigenvalues indicate a presence of the instability, which in turn implies the existence of one or more BS HF solutions with lower energy than the SA one. A detailed derivation of singlet, triplet or more general stability conditions can be found in references [2,3,6] and references therein (for a review see Refs. [7–9]).

It should be stressed that the energy lowering due to a singlet instability is generally much smaller than the energy lowering implied by a triplet instability. While the triplet instabilities are rather common, at least for the systems with stretched chemical bonds, the singlet instabilities are much less frequent and represent, in fact, a rather surprising phenomenon. Their physical or chemical interpretation is far from being straightforward. Yet, at the HF level, a broken space-symmetry HF solution that is associated with a singlet instability of the SA RHF solution invariably implies the tendency of the (otherwise frozen) nuclear framework to distort accordingly. In some cases this distortion persists even at the post-HF correlated level (see, e.g., Ref. [10]), while in other cases this tendency is artificial and is overcome when a better approximation is used (e.g., Ref. [11]; see also Ref. [8]). This phenomenon may be regarded as an example of a spontaneous symmetry breaking in molecular systems, analogously as in the low-density electron gas or in the spontaneous magnetization in the infinite ferromagnets. We recall that in the case of atoms, the breaking of spherical symmetry indicates a tendency towards autoionization or, in general, a physical instability of a given system [12,13].

The singlet unstable RHF solutions have been found in a number of molecular systems at both semiempirical and ab initio levels (for an overview, see Refs. [8,9]). A number of seemingly hypothetical structures does actually exist and has been the subject of many experimental investigations (such as polyacetylene films, alkali metal and gold nanowires, metal clusters etc.).

The above outlined stability problem is, of course, pertinent to any variational solution that imposes constraints on the variational wave function, be they of a symmetry or other nature. Thus, the same kind of spin and/or space symmetry breaking also arises in nowadays widely used density functional theory (DFT), (using either Kohn-Sham (KS) or local density approximation (LDA), see, e.g., Refs. [14–17]), be it applied to molecular electronic structure [18,19], solid state [15,16,20] or other systems (such as metal clusters [15] or quantum dots [17,21]). Indeed, a general classification of HF instabilities due to Fukutome [6] applies to DFT solutions as well [22]. The presence or absence of instabilities in DFT is very much dependent on the employed functional. The tendency towards instabilities is, generally, less pronounced in DFT than in the standard HF approaches, since it implicitly accounts for correlation effects [19].

In this paper we wish to address the phenomenon that can be loosely characterized as an "approximate" symmetry breaking, namely the tendency of the charge density waves (CDWs) that arise due to the symmetry breaking in highly symmetric systems (such as cyclic polyenes or infinite linear metals) to persist even in similar systems of lower or no spatial symmetry. For this purpose we consider cyclic polyenes C_NH_N with a nondegenerate ground state, $N = 4\nu + 2$, and their distorted versions, in particular π-electron models of the so-called $[n]$-annulenes, which may also be viewed as the perimeter models (or p-models for short) of aromatic hydrocarbons, in our case of linear polyacenes. For easier reference, as well as to emphasize the model nature of the considered systems, we refer to the latter as p-polyacenes (specifically, p-naphthalene and p-anthracene, the letter "p" indicating the "perimeter" model of these systems). Thus, starting with highly symmetric cyclic polyenes $C_{10}H_{10}$ and $C_{14}H_{14}$, forming a regular N-gon ($N = 10$ and 14), whose HF solution is fully determined by their D_{Nh} symmetry group, we systematically deform the nuclear framework while preserving the C–C bond lengths, until we reach the corresponding p-polyacenes having the D_{2h} symmetry. The basic qualitative observations described below for p-naphthalene and p-anthracene have been extended to much larger p-polyacenes, as well as to other aromatic hydrocarbons with D_{1h}, D_{3h} or D_{6h} symmetry, including the description of other features of these systems and a comparison with existing annulenes [23].

In Section 2 we briefly describe the Pariser-Parr-Pople Hamiltonian that is employed in this study and in Section 3 we recall some basics theorems concerning HF solutions in the fully correlated limit ($\beta = 0$), which are helpful in interpreting our results, presented in Section 4. Concluding remarks are then given in Section 5.

2 Pariser-Parr-Pople Hamiltonian

We employ a semiempirical Pariser-Parr-Pople (PPP) Hamiltonian [24,25] which was initially developed for the description of planar π-electron systems with conjugated double bonds. This Hamiltonian represents a generalization of the Hubbard Hamiltonian – that is often used in solid-state physics – since it replaces the on-site Coulomb interaction of the latter by a more realistic long-range interaction. Its general form is (see, e.g., Ref. [25])

$$\begin{aligned} H_{\mathrm{PPP}} = &\sum_{\mu} \alpha_{\mu} + {\sum_{\mu,\nu}}' \beta_{\mu\nu} E_{\mu\nu} \\ &+ \sum_{\mu<\nu} \gamma_{\mu\nu} (E_{\mu\mu} - Z\mu)(E_{\nu\nu} - Z\nu) \\ &+ \frac{1}{2} \sum_{\mu} \gamma_{\mu\mu} E_{\mu\mu} (E_{\mu\mu} - 1), \end{aligned} \tag{3}$$

where the summation indices μ and ν label the atomic sites of the system, the prime on the second summation symbol indicates that the sum extends only over the σ-bonded nearest neighboring sites (the tight-binding approximation), α_{μ} and $\beta_{\mu\nu}$ are the so-called Coulomb and resonance (or hopping) one-electron integrals, and $\gamma_{\mu\nu} \equiv \langle \mu\nu|v|\mu\nu\rangle$ represents the two-electron Coulomb integral involving sites μ and ν. Further, Z_{μ} designates the number of π-electrons contributed by the μth atomic site (for neutral, unsaturated hydrocarbons with conjugated double bonds $Z_{\mu} = 1$). Finally, the operators $E_{\mu\nu}$ represent the generators of the orbital unitary group $\mathrm{U}(N)$, with N designating the number of atomic sites and of the corresponding symmetrically-orthonormalized $2p_z$ carbon atomic spinorbitals $|\mu\sigma\rangle$, $\mu = 1, \cdots, N$ and $\sigma = \pm\frac{1}{2}$ (see Ref. [25] for more details), namely

$$E_{\mu\nu} = \sum_{\sigma} X^{\dagger}_{\mu\sigma} X_{\nu\sigma}, \tag{4}$$

with $X^{\dagger}_{\mu\sigma}$ ($X_{\nu\sigma}$) designating the creation (annihilation) operators defined on the spin-orbital set $\{|\mu\sigma\rangle\}$.

In the case of neutral hydrocarbons the one-center integrals are all identical, i.e. $\alpha_{\mu} \equiv \alpha$ and $\gamma_{\mu\mu} \equiv \gamma_{11}$, so that without any loss of generality we can define the origin of our energy scale by setting $\alpha = 0$, and thus simplify the PPP Hamiltonian as follows [25,26]:

$$H_{\mathrm{PPP}} = {\sum_{\mu,\nu}}' \beta_{\mu\nu} E_{\mu\nu} + \frac{1}{2} \sum_{\mu\nu} \gamma_{\mu\nu} E_{\mu\mu} (E_{\nu\nu} - 1). \tag{5}$$

Moreover, since all the C–C bondlengths in our model are kept identical, all the $\beta_{\mu\nu}$ integrals are the same, so that we can set $\beta_{\mu\nu} \equiv \beta$. Thus, the semiempirical parameters specifying the PPP Hamiltonian are reduced to the resonance integral β, whose spectroscopic value is usually set to –2.4 eV, and the two-electron Coulomb integrals $\gamma_{\mu\nu}$. For the latter, we employ the Mataga-Nishimoto parametrization [27], representing essentially a point-charge Coulomb interaction between the electrons on sites μ and ν, modified in such a way that for the on-site interaction we obtain γ_{11}, whose value is given by the difference between the valence state ionization potential and electron affinity for the $2p_z$ carbon atomic orbital (Goeppert-Mayer and Sklar approximation). We thus have that $\gamma_{11} = 10.84$ eV, while the other Coulomb-repulsion integrals are given by the formula

$$\gamma_{\mu\nu}(R_{\mu\nu}) = \frac{e^2}{R_{\mu\nu} + a}, \tag{6}$$

where $a = \frac{e^2}{\gamma_{11}}$. This approximation represents an interpolation between the finite γ value for $R_{\mu\nu} = 0$ and the standard point-charge Coulomb repulsion for $R_{\mu\nu} \to \infty$. We note that by setting $\gamma_{\mu\nu} = 0$ for $\mu \neq \nu$ and $\gamma_{11} = U$, we obtain the Hubbard Hamiltonian. The studied systems can then be explored in the whole range of the coupling constant (proportional to $\frac{1}{\beta}$) by varying the resonance integral β from 0 to $-\infty$ (in actual calculations reached at about –5 eV, the physical region corresponding to the spectroscopic value of $\beta = -2.4$ eV), while keeping the $\gamma_{\mu\nu}$ integrals fixed.

3 Some basics theorems

Let us first recall some simple theorems [4] for π-electron systems with conjugated double bonds which a priori tell us whether the singlet instability can, in principle, arise for sufficiently large coupling constants or whether the RHF solution for a given system will always be stable.

We start with the definition of *Kekulé* or *Dewar solutions* that are associated with the corresponding valence-bond (VB) structures. These are formed by introducing n "bonds" between all possible $2n$ atomic sites of a system with conjugated double bonds. For Kekulé VB structures these bonds occur only between σ-bonded nearest neighbors. The wave function Φ that we associate with each VB structure is then represented by a single antisymmetrized product of n doubly occupied ethylene-like molecular orbitals ψ_i,

$$|\psi_i\rangle = (|\mu(i)\rangle + |\nu(i)\rangle)/\sqrt{2}, \tag{7}$$

where $\mu(i)$ and $\nu(i)$ label the sites associated with the ith bond of a given VB structure. Clearly, $|\mu\sigma\rangle = |\mu\rangle|\sigma\rangle$. Thus

$$\Phi = \det \|\psi_1\alpha, \psi_1\beta, \psi_2\alpha, ..., \psi_n\beta\|, \tag{8}$$

with α and β now labeling the spin-up ($\sigma = \frac{1}{2}$) and spin-down ($\sigma = -\frac{1}{2}$) functions, respectively. With these definitions in hand, the relevant basic properties of the Kekulé and Dewar solutions Φ in the fully correlated limit ($\beta = 0$) can be characterized as follows [4].

Theorem 1. *Any Kekulé or Dewar solution represents an exact RHF solutions in the fully correlated limit of* $\beta = 0$.

Theorem 2. *The total* π*-electron energy of any Dewar solution is higher than the energy of any Kekulé solution.*

Theorem 3. *In the fully correlated limit* $\beta = 0$*, all Kekulé solutions are degenerate and their energy represents the*

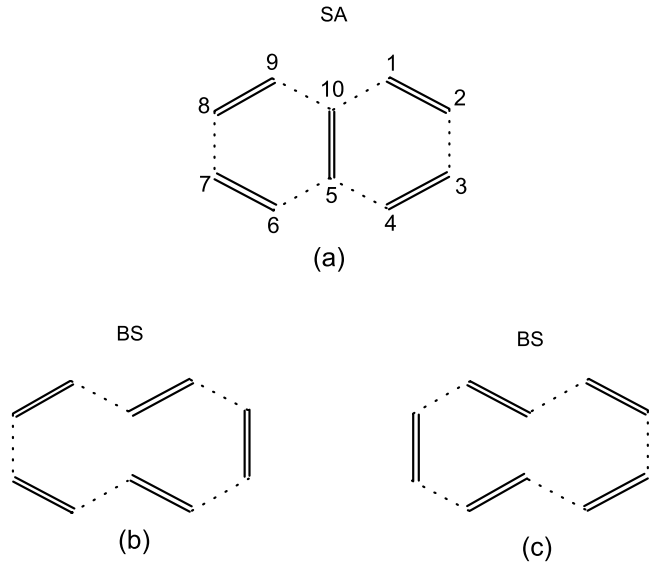

Fig. 1. The structure (a) describes the SA RHF solution for p-naphthalene in the fully correlated limit ($\beta = 0$). For this structure the site numbering is also indicated. Diagrams (b) and (c) then correspond to two possible Kekulé structures representing degenerate BS solutions in the fully correlated limit.

absolute minimum of the energy in the variational space that is spanned by all single determinantal wave functions with doubly occupied orbitals.

These theorems can be easily proved as shown in the appendix of reference [4]. Theorem 3 then implies that if any SA RHF solution for $\beta = 0$ has the form of a Kekulé solution Φ, equations (7) and (8), it must necessarily be singlet stable in the whole range of the coupling constant, since the nonzero one-body component of the Hamiltonian (i.e., non-zero β) can only increase its stability. This in turn leads to the following Corollary.

Corollary. *Let the symmetry of the π-electron Hamiltonian of a system with conjugated double bonds be characterized by a point group G. If there exists a Kekulé structure having the same point group symmetry G, then the SA RHF solution of a given system is always stable. However, if all the Kekulé structures have a lower symmetry G', where G' designates a proper subgroup of G, then the SA RHF solution may become singlet unstable in some region of the coupling constant, namely for $0 \leq |\beta| \leq |\beta_{\rm crit}|$.*

4 Results

Let us first point out the implications of the above stated theorems for the case of p-naphthalene and p-anthracene. The SA solution for p-naphthalene in the fully correlated limit ($\beta = 0$) is shown schematically in Figure 1a. It represents a fully symmetric D_{2h} solution, which is an exact RHF solution for $\beta = 0$ (see Th. 1). It is important to note here that for $\beta = 0$ the Hamiltonians for the p-naphthalene and an ordinary naphthalene are identical. This explains the presence of the strong bond across the ring. The two Kekulé structures for p-naphthalene, shown in Figures 1b and 1c, then correspond to BS RHF solutions. All three solutions are degenerate at $\beta = 0$ (see Th. 3).

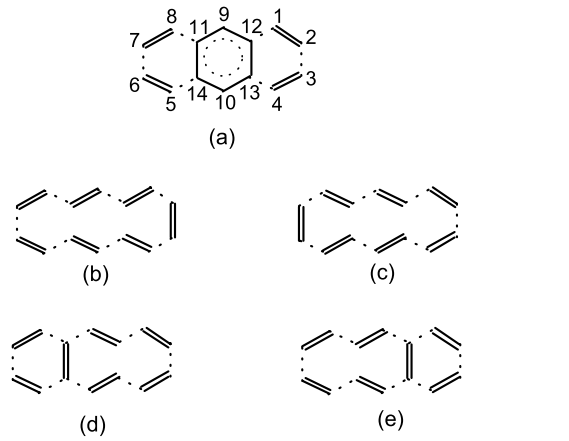

Fig. 2. The structure (a) describes the SA RHF solution for p-anthracene in the fully correlated limit. For this structure the site numbering used in the text is shown. The Kekulé structures (b)–(e) then represent degenerate BS solutions for this system in the fully correlated limit.

The corresponding picture for p-anthracene is shown in Figure 2. The SA RHF solution at $\beta = 0$ is now schematically represented in Figure 2a and will be discussed later on. The solutions shown in Figures 2b–2e then represent all possible Kekulé solutions for p-anthracene at $\beta = 0$. Clearly, none of these structures possesses the D_{2h} symmetry of the Hamiltonian, since these structures, and the corresponding RHF solutions, have broken C_{2v} symmetry. Consequently, the SA RHF solution may become unstable for some values of β (see the Corollary).

A similar situation is found for cyclic polyenes $C_N H_N$ for any $N = 2n = 4\nu{+}2$, in which case no Kekulé structure has the D_{Nh} symmetry of the Hamiltonian (or of the corresponding SA RHF solution), but has a lower D_{nh} symmetry instead. This is illustrated for $C_{10}H_{10}$ in Figure 3. Thus, the SA RHF solution for these systems is bound to become singlet unstable in some interval $0 \leq |\beta| \leq |\beta_{\rm crit}|$ of the resonance integral β.

The SA RHF solutions for linear polyacenes are always singlet stable when they involve an even number of benzene rings, since these systems possess a fully symmetric D_{2h} Kekulé structure (see Ref. [4] and the Corollary), while the opposite is the case for linear polyacenes having an odd number of benzene rings. Thus, the SA RHF solutions for naphthalene, having two benzene rings, are always singlet stable, while for anthracene, with three benzene rings, there will be a region $0 \leq |\beta| \leq |\beta_{\rm crit}|$ of singlet instability. As we shall see later on, we find a rather different behavior for the corresponding perimeter models (p-polyacenes), even though the qualitatively different nature of the SA RHF solutions for linear polyacenes having an even or an odd number of benzene rings will also be reflected in the behavior of their p-versions, particularly in the vicinity of the fully correlated limit $\beta = 0$. In view of a qualitatively different behavior of the RHF solutions

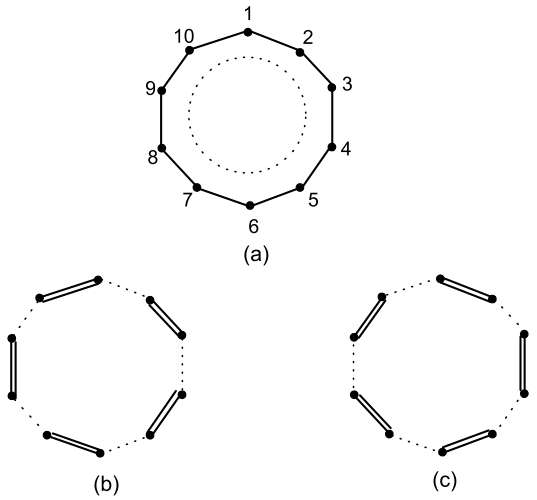

Fig. 3. The structure (a) describes the SA RHF solution for the $C_{10}H_{10}$ cyclic polyene in the whole range of the coupling constant, including the fully correlated limit. The Kekulé structures (b) and (c) then represent two degenerate BS solutions in the fully correlated limit.

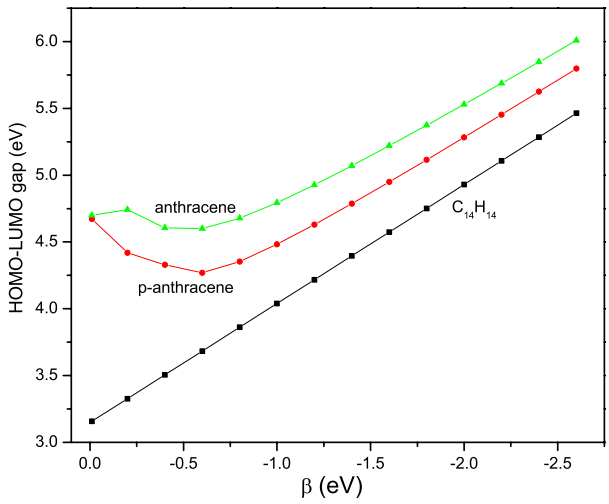

Fig. 4. (Color online) The energy gaps between the highest occupied and the lowest unoccupied molecular orbitals (HOMO-LUMO gaps) for anthracene, p-anthracene, and the $C_{14}H_{14}$ cyclic polyene as a function of the resonance integral β.

for linear polyacenes having an even or an odd number of benzene rings, we shall refer to them as even and odd polyacenes, respectively. For the simplicity's sake, we will also use the same terminology for their p-analogues, while referring to cyclic polyenes simply as polyenes.

Moreover, we have shown in reference [23] that there is only a very slight dependence of $|\beta_{\rm crit}|$ on the size N of polyacenes ($|\beta_{\rm crit}|$ being practically constant when increasing N), while $|\beta_{\rm crit}|$ increases rapidly with increasing N for p-polyacenes, and even more rapidly for polyenes (reaching the spectroscopic value of β for $N \approx 34$ and 26, respectively; see Fig. 2 of Ref. [23]). In general we have that

$$|\beta_{\rm crit}({\rm polyacene})| < |\beta_{\rm crit}({\rm p-polyacene})| < |\beta_{\rm crit}({\rm polyene})|. \quad (9)$$

This fact is necessarily reflected in the energy gap between the highest occupied and the lowest unoccupied orbital energies (HOMO-LUMO gap) of the respective SA solutions. This is illustrated in Figure 4 where we plot the HOMU-LUMO gap for anthracene, p-anthracene, and $C_{14}H_{14}$ as a function of β. A much stronger tendency towards instability for the $N = 14$ polyene as compared with the other two systems is clearly related to its much smaller HOMO-LUMO gap. We also observe that in the $\beta = 0$ limit, the HOMO-LUMO gaps for anthracene and p-anthracene become identical, since there is no difference between their π-electron Hamiltonians in this limit, as already pointed out above.

It can also be shown that the energy difference $\Delta E = E_0^{\rm SA} - E_0^{\rm BS}$ between the energies of the SA and BS RHF solutions, which is defined and positive in the region of singlet instability (since the BS solution has a lower energy than the SA one), monotonically increases with decreasing $|\beta|$ for polyenes, reaching its maximum at $\beta = 0$. However, for distorted polyenes we find a different behavior. Although initially, starting at $\beta_{\rm crit}$, the energy difference ΔE increases with decreasing $|\beta|$ value, it eventually reaches its maximum and decreases towards zero at $\beta = 0$ in the case of p-naphthalene, while reaching a finite value at $\beta = 0$ for p-anthracene, which is identical with that for anthracene (see Fig. 5). This behavior is easily understood when we realize that at $\beta = 0$ the Hamiltonians for polyacenes and their perimeter analogues are identical, and that the SA RHF solutions for even polyacenes is always stable and its energy at $\beta = 0$ is given by any Kekulé structure [23].

Another interesting feature is revealed when we consider the dependence of the lowest root $\lambda_{\rm min}$ of the singlet stability problem for the SA RHF solution on the resonance integral β (see Fig. 6). While for $N = 10$ polyene $\lambda_{\rm min}$ decreases linearly with $|\beta|$, reflecting an increasing instability of the SA solution when approaching the fully correlated limit, for p-naphthalene we find a region near $\beta = 0$ where no singlet instability is present. In order to understand this peculiar behavior of the SA RHF solutions for p-naphthalene, it is instructive to examine the mean-energy hypersurface $E(\Phi)$, equation (1), for different values of the resonance integral β. This energy hypersurface for both the $N = 10$ polyene and p-naphthalene is schematically represented in Figure 7 as a one-dimensional plot along a hypothetical coordinate in the variational manifold passing through the BS and SA solutions. The lowest root $\lambda_{\rm min}$ may be though of as representing the curvature of the respective stationary points along this coordinate.

Considering first the $C_{10}H_{10}$ polyene, we find that at $\beta = 0$ we have two degenerate BS solutions (indicated by 1 and 2 in Fig. 7 and depicted in Fig. 3, diagrams 3b and 3c), as well as the unstable SA solution (designated by 0 in Fig. 7 and depicted in Fig. 3a), separated by the energy difference of approximately 1.01 eV. The respective solutions are best characterized by the corresponding bond

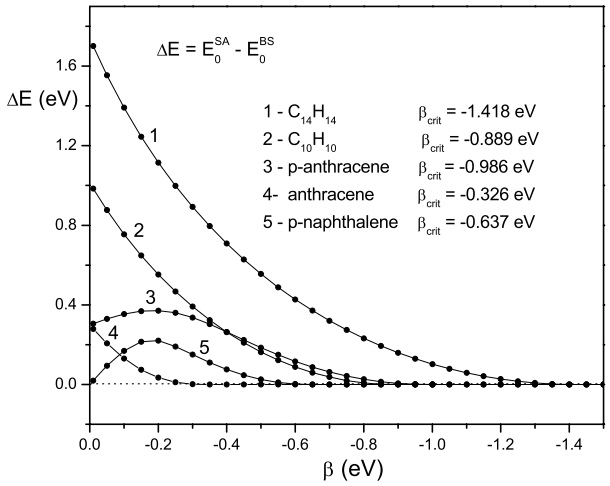

Fig. 5. The energy difference $\Delta E = E_0^{\rm SA} - E_0^{\rm BS}$ between the SA and BS solutions for various structures as a function of the resonance integral β. The curves 1 and 2 correspond to the $C_{14}H_{14}$ and $C_{10}H_{10}$ cyclic polyenes, respectively. The curves 3 and 4 correspond, respectively, to p-anthracene and anthracene, and merge into a common finite value in the fully correlated limit. For p-naphthalene (curve 5) ΔE vanishes for $\beta = 0$. The critical values $\beta_{\rm crit}$ are also listed in the figure for each case. See the text for details.

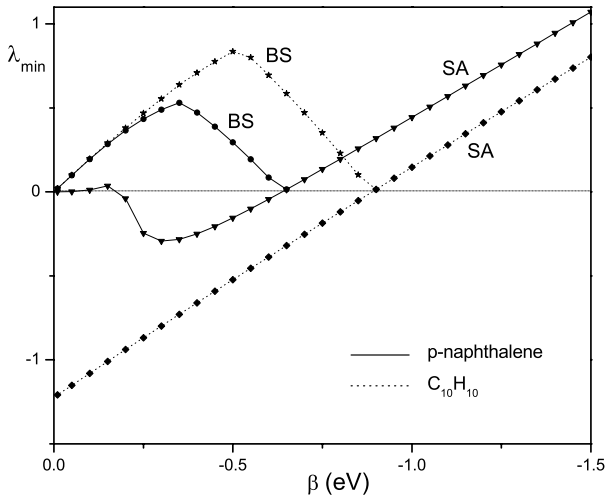

Fig. 6. The dependence of the lowest-lying roots $\lambda_{\rm min}$ of the singlet stability problem for the SA and BS solutions of p-naphthalene (full lines) and $C_{10}H_{10}$ cyclic polyene (dotted lines) as a function of the resonance integral β. In each case the curves corresponding to the BS and SA solutions merge at the critical value of the resonance integral $\beta_{\rm crit}$ (see Fig. 5). For $|\beta| > |\beta_{\rm crit}|$ only SA solutions exist.

orders $p_{\mu,\nu}$,

$$p_{\mu,\nu} = 2\sum_i \overline{C}_{i,\mu} C_{i,\nu}, \tag{10}$$

where the sum extends over all occupied molecular orbitals (MOs) and $C_{i,\mu}$ designates the coefficient in the expansion of the MO ψ_i in terms of the atomic orbitals (AOs) $\chi_\mu \equiv \langle r|\mu\rangle$,

$$\psi_i = \sum_\mu C_{i,\mu}\chi_\mu. \tag{11}$$

Since the MOs of the highly-symmetric $C_{10}H_{10}$ polyene are fully determined by its D_{10h} symmetry for any value of β, all the bond orders have the same constant value $p_{\mu,\mu\pm1} = 0.64$, $\mu = 1, \cdots, N (\mathrm{mod}\ N)$. When $|\beta|$ increases, the energy difference between the two degenerate BS solutions and the SA solution decreases, and vanishes at $|\beta| = |\beta_{\rm crit}| = 0.889$ eV, at which point the SA solution becomes stable. For $|\beta| > |\beta_{\rm crit}|$ only this SA solution exists.

For p-naphthalene the circumstances are more involved. At $\beta = 0$, the two BS solutions (labeled as 1 and 2 in Fig. 7; see also Figs. 1b and 1c) and the SA solution (designated by 0 in Fig. 7, see also Fig. 1a) are all degenerate. As we proceed from the fully correlated limit by increasing the $|\beta|$ value, the SA solution remains stable ($\lambda_{\rm min} > 0$) till about $\beta \approx -0.2$ eV, when the local minimum corresponding to the SA solution disappears and changes into a local maximum (i.e., $\lambda_{\rm min}$ becomes negative), so that for $|\beta| \gtrsim 0.2$ eV the SA solution becomes unstable as in the polyenic case. With a further increase of $|\beta|$ the energy difference between the SA and BS solutions steadily diminishes in much the same way as for the corresponding polyene (cf. Fig. 7), and for

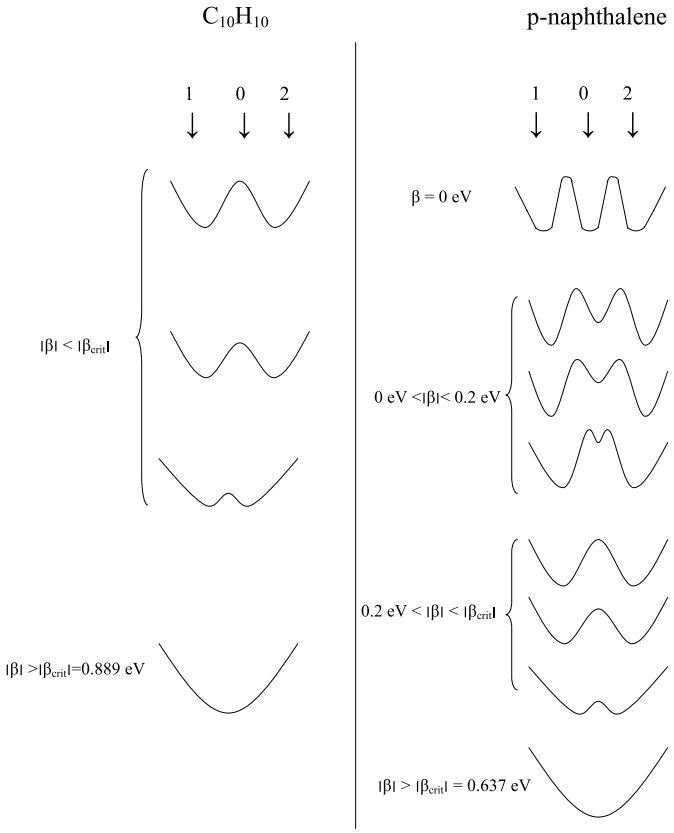

Fig. 7. A schematic representation of the cut of the variational mean-energy hypersurface $E(\Phi)$, equation (1), passing through the two degenerate BS solutions (labeled by 1 and 2) and the SA solution (labeled by 0) of the $C_{10}H_{10}$ cyclic polyene (left panel) and of p-naphthalene (right panel) for typical values of the resonance integral β. See the text for details.

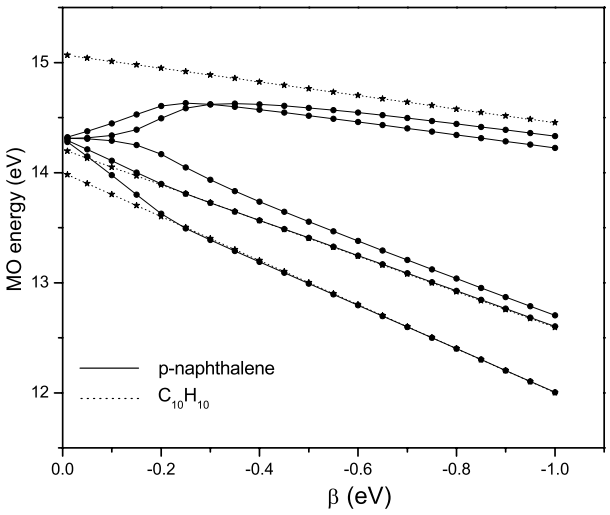

Fig. 8. Energies of occupied RHF molecular-orbitals of p-naphthalene (full lines) and of the $C_{10}H_{10}$ cyclic polyene (dotted lines) as a function of the resonance integral β. Note that due to the D_{10h} symmetry of the $C_{10}H_{10}$ cyclic polyene there is a double degeneracy of the two highest molecular orbitals. This degeneracy is lifted in p-naphthalene.

$|\beta| > |\beta_{\rm crit}| = 0.637$ eV the BS solutions disappear altogether and only the SA solution exists. Thus, as the π-electron Hamiltonian for p-naphthalene approaches that of naphthalene when $\beta \to 0$, not only the energy difference $\Delta E = E_0^{\rm SA} - E_0^{\rm BS}$ for p-naphthalene tends to zero, but also the SA solution for p-naphthalene stabilizes within a small neighborhood of the fully correlated limit.

The above presented results clearly demonstrate that a deformation of the nuclear framework of cyclic polyenes has interesting consequences in the region of small values of β. Of course, we will observe the same phenomenon even for physical (spectroscopic) values of parameters once we consider larger systems, as implied by the fact that the critical value of $|\beta|$ steadily increases with increasing size of the polyenes N. The above presented phenomena are also reflected in the behavior of the MO energies (see Fig. 8 for occupied MOs). For $N = 10$ polyene these MO energies depend linearly on β, while those for p-naphthalene approach the same value of 14.3 eV as $\beta \to 0$. This can be understood when we realize that at $\beta = 0$ the SA solution for p-naphthalene factorizes into the five ethylene-like solutions, so that the energy of all five occupied MOs of p-naphthalene approaches the energy of the single occupied ethylenic MO, whose orbital energy is precisely 14.3 eV (and similarly for the corresponding virtual MOs). For large values of $|\beta|$, the two-electron component of the Hamiltonian plays less and less important role as it approaches the Hückel uncorrelated limit and the MO energies behave in the same way as for highly symmetric polyenes (note that the geometry of the nuclear framework is irrelevant in the Hückel limit, where only the topological incidence matrix is decisive).

It remains to clarify the behavior that is observed for p-anthracene as the system approaches anthracenic structure in the $\beta \to 0$ limit and, in particular, the earlier mentioned character of its SA solution in this limit. We already know that anthracene, with its odd number (i.e., three) of benzene rings, has a nonvanishing region of singlet instability for its SA RHF solution. The lowest root $\lambda_{\rm min}$ of the p-anthracene stability problem, shown in Figure 9 as a function of $|\beta|$, remains negative for $|\beta| < |\beta_{\rm crit}| = 0.986$ eV as we approach the fully correlated limit, even though its dependence on $|\beta|$ is not monotonic as in the case of $N = 10$ polyene.

In order to elucidate the character of the SA solution for p-anthracene in the fully correlated limit, we present in Table 1 the values of essential bond orders (for the site numbering see Fig. 2a) for both the SA and BS solutions for several values of β in the neighborhood of the fully correlated limit. We see that at $\beta = 0$ the SA solution factorizes into a benzene-like solution (cf. bond orders $9{,}12_{sa}$ and $12{,}13_{sa}$) and four ethylene-like solutions, as indicated schematically in Figure 2a. This also explains why we find a finite energy difference $\Delta E \approx 0.3$ eV at $\beta = 0$, since this is the energy difference between the energy of a BS solution of benzene with alternating bond orders of magnitude 0 and 1 and the energy of a SA solution of benzene with constant bond orders $p_{\mu,\mu\pm1} = 0.66$. Since at $\beta = 0$ the π-electron Hamiltonians of anthracane and p-anthracene are identical, the energy difference between the SA and BS solutions of anthracene goes to the same value $\Delta E \approx 0.3$ eV.

We observe that, in general, the behavior of the π-electron energy of SA and BS solutions for various p-versions of polyacenes depends critically on the evenness or oddness of the number of constituting benzene rings. Those with an even number of rings behave very much like the above presented case of naphthalene and p-naphthalene, whose SA solutions at $\beta = 0$ coincide and are characterized by the symmetric Kekulé structure, while those with an odd number of benzene rings, exemplified by anthracene and p-anthracene, tend towards a "quasi-Kekulé" structure at $\beta = 0$ with the benzenoid ring in the middle that is surrounded by ethylenic fragments [23].

5 Conclusions

In this work we examine the symmetry breaking effects at the Hartree-Fock level of approximation for the π-electron models of p-naphthalene and p-anthracene, which result by a systematic deformation of the nuclear framework of highly symmetric $C_{10}H_{10}$ and $C_{14}H_{14}$ cyclic polyenes. Similar properties for cyclic polyenes C_NH_N, $N = 4\nu + 2$, were thoroughly investigated in several papers earlier (cf., e.g., Refs. [2,7]). In this case the SA RHF solutions become singlet unstable for sufficiently small values of the resonance integral $|\beta|$, which steadily increases with the size of the polyene ring N, implying the existence of BS RHF solutions with lower energy. Those BS solutions having the lowest energy possess the D_{nh}, $n = N/2$, symmetry and are characterized by alternating bond orders (see Figs. 3b and 3c).

Let us recall that the existence of the above mentioned BS solutions implies a tendency towards the actual

Table 1. Bond orders $p_{\mu,\nu}$ of the SA solution (denoted as μ,ν_{sa}) and of the BS solution (μ,ν_{bs}) of p-anthracene for several values of the resonance integral β (in eV) in the range of singlet instability ($\beta_{\rm crit} = -0.986$ eV). The labeling of bonds is shown in Figure 2a.

β	$9{,}12_{sa}$	$1{,}12_{sa}$	$1{,}2_{sa}$	$2{,}3_{sa}$	$12{,}13_{sa}$	$9{,}12_{bs}$	$1{,}12_{bs}$	$1{,}2_{bs}$	$2{,}3_{bs}$	$12{,}13_{bs}$	$9{,}11_{bs}$	$8{,}11_{bs}$	$7{,}8_{bs}$	$6{,}7_{bs}$	$11{,}14_{bs}$
−0.5	0.647	0.530	0.760	0.545	0.371	0.930	0.264	0.922	0.304	0.068	0.264	0.898	0.355	0.887	0.201
−0.4	0.655	0.471	0.810	0.483	0.426	0.951	0.222	0.943	0.261	0.043	0.220	0.927	0.301	0.917	0.162
−0.3	0.667	0.365	0.884	0.371	0.504	0.969	0.178	0.962	0.214	0.023	0.176	0.953	0.241	0.946	0.117
−0.2	0.676	0.232	0.951	0.237	0.577	0.983	0.129	0.979	0.160	0.009	0.128	0.966	0.173	0.971	0.069
−0.1	0.677	0.109	0.988	0.113	0.628	0.995	0.072	0.993	0.092	0.001	0.072	0.993	0.096	0.991	0.024
−0.001	0.667	0.001	1	0.001	0.666	1	0.001	1	0.001	0	0.001	1	0.001	1	0

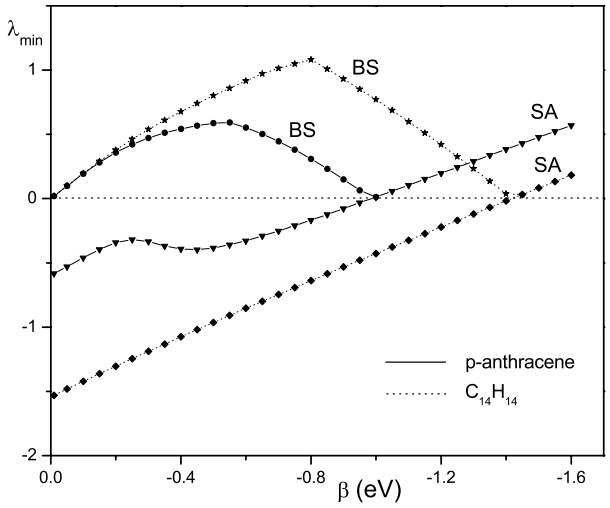

Fig. 9. The dependence of the lowest-lying roots $\lambda_{\rm min}$ of the singlet stability problem for the SA and BS solutions of p-anthracene (full lines) and $C_{14}H_{14}$ cyclic polyene (dotted lines) as a function of the resonance integral β.

distortion of the nuclear framework in which the C–C bond lengths are no longer identical [28]. Indeed, one can show [8,28] that a distortion that is "in-phase" with the charge density wave (as given by the bond-order matrix) of one of the BS solutions will further lower the energy, while the "out-of-phase" one will increase it. Thus the resulting potential energy curve (PEC) as a function of the distortion parameter Δ (given, e.g., by the difference between the alternating longer and shorter C–C bond lengths in a distorted structure) will have a finite slope at the undistorted geometry $\Delta = 0$, and the two PECs associated with two modes of distortion that correspond to the two degenerate BS solutions will intersect at a finite angle, forming a double well PEC [8,28]. Since $|\beta_{\rm crit}|$ increases rapidly with the increasing number of atomic sites N, reaching its physical (spectroscopic) value of about −2.4 eV for $N \approx 26$ or 30 (depending on the parametrization employed), this phenomenon implies the actual distortion or bond-length alternation in long polyenic chains as experimentally observed in polyacetylene. Indeed, adding the σ-energy component, one arrives to an experimentally determined distortion of $\Delta \approx 0.04$ or 0.05 Å [8,28].

Both p-naphthalene and p-anthracene have D_{2h} symmetry and result by a distortion of the D_{Nh} polyenes with $N = 10$ and 14, respectively. In general, a lowering of the symmetry of the nuclear framework brings about a lowering of the critical value $|\beta_{\rm crit}|$, i.e., the region of the β values in which the singlet unstable SA RHF (and thus BS) solutions exist is significantly smaller than for polyenes, yet much larger than for the corresponding odd polyacenes (even polyacenes being always stable). Nonetheless, this region of instability persists as long as there remains some symmetry to be broken [23].

We find that in contrast with the $C_{10}H_{10}$ cyclic polyene, in which case the energy difference between the BS and SA solutions monotonically increases when we approach the fully correlated limit, this energy difference vanishes at $\beta = 0$ in the case of p-naphthalene (see Fig. 5). This is related to the fact that the SA RHF solutions for even polyacenes are always stable. Moreover, the SA solution for p-naphthalene stabilizes in the vicinity of the fully correlated limit (see Fig. 6), again in contrast to the $N = 10$ polyene, in which case the singlet instability of its SA solution persists all the way to the fully correlated limit. Similar conclusions hold for the p-versions of larger polyacenes.

An entirely different situation is found for anthracene, representing odd polyacenes, and for its p-analogue. The SA RHF solutions for both systems are singlet unstable in the finite region $0 \leq |\beta| \leq |\beta_{\rm crit}|$, and the energy difference $\Delta E = E_0^{\rm SA} - E_0^{\rm BS}$ between the SA and BS solutions for p-anthracene tends towards the same finite value of 0.3 eV when $\beta \to 0$ as does ΔE for anthracene (see Fig. 5). Indeed, this is the same energy difference ΔE that is found between the SA solution for benzene (characterized by constant bond orders $p_{\mu,\mu\pm1} = \frac{2}{3}$, see Fig. 2) and the BS solution consisting of three ethylenic fragments (characterized by alternating bond orders 0 and 1). Again, we find the same results for larger odd polyacenes and p-polyacenes [23]. Since no D_{2h} Kekulé structure exists for these systems, the SA solution in the fully correlated limit always consists of a central benzenic ring surrounded by ethylenic fragments. Consequently, the energy difference ΔE at $\beta = 0$ for odd polyacenes and p-polyacenes is always the same, regardless the size of the system [23].

In summary, the study of cyclic polyenes and of their distorted versions, particularly those representing perimeter models of linear polyacenes (p-polyacenes), shows the essential role played by the symmetry when exploring their respective BS and SA RHF solutions and their properties. A more detailed study in reference [23] reveals that quite unexpected properties of those solutions propagate to much larger hydrocarbons with conjugated

double bonds. Moreover, a seemingly hypothetical structures like p-polyacenes do actually exist, since their geometric framework can be stabilized with methylenic or similar bridges, and many of these so-called [n]-annulenes were studied in great detail experimentally. For the relevance of our study for a better understanding of these systems we refer the reader to reference [23].

Continued support by NSERC (J.P.) is gratefully acknowledged.

References

1. D.J. Thouless, *The Quantum Mechanics in Many-Body Systems* (Academic, New York, 1961)
2. J. Čížek, J. Paldus, J. Chem. Phys. **47**, 3976 (1967)
3. J. Paldus, J. Čížek, J. Chem. Phys. **52**, 2919 (1970); Chem. Phys. Lett. **3**, 1 (1969)
4. J. Čížek, J. Paldus, J. Chem. Phys. **53**, 821 (1970)
5. P.-O. Löwdin, Rev. Mod. Phys. **35**, 496 (1963); P.-O. Löwdin, Adv. Chem. Phys. **14**, 283 (1969)
6. H. Fukutome, Int. J. Quantum Chem. **20**, 955 (1981)
7. J. Paldus, J. Čížek, Phys. Rev. A **2**, 2268 (1970) and references therein
8. J. Paldus, in *Self-Consistent Field: Theory and Applications*, edited by R. Carbó, M. Klobukowski (Elsevier, Amsterdam, 1990), pp. 1–45
9. J.L. Stuber, in *Fundamental World of Quantum Chemistry, A Tribute Volume to the Memory of Per-Olov Löwdin*, edited by E.J. Brändas, E.S. Kryachko (Kluwer, Dordrecht, The Netherlands, 2003), Vol. 1, pp. 67–139
10. X. Li, J. Paldus, J. Chem. Phys. **126**, 224304 (2007)
11. J. Paldus, A. Veillard, Chem. Phys. Lett. **50**, 6 (1977); J. Paldus, A. Veillard, Mol. Phys. **35**, 445 (1978)
12. J. Paldus, J. Čížek, Can. J. Chem. **63**, 1803 (1985); T.A. Kaplan, W. Kleiner, Phys. Rev. **156**, 1 (1967)
13. F. Holka, P. Neogrády, M. Urban, J. Paldus, Collect. Czech. Chem. C **72**, 197 (2007)
14. I.G. Kaplan, Int. J. Quantum Chem. **107**, 2595 (2007)
15. F.W. Averill, G.F. Painter, Phys. Rev. B **46**, 2498 (1992)
16. A.I. Liechtenstein, V.I. Anisimov, J. Zaanen, Phys. Rev. B **52**, R5467 (1995)
17. A. Harju, E. Räsänen, H. Saarikoski, M.J. Puska, R.M. Nieminen, K. Niemelä, Phys. Rev. B **69**, 153101 (2004)
18. J.M. Wittbrodt, H.B. Schlegel, J. Chem. Phys. **105**, 6574 (1996); C.D. Sherill, M.S. Lee, M. Head-Gordon, Chem. Phys. Lett. **302**, 425 (1999); M. Filatov, S. Shaik, Chem. Phys. Lett. **332**, 409 (2000)
19. M. Alcami, O. Mó, M. Yáñez, I.L. Cooper, J. Chem. Phys. **112**, 6131 (2000); G. Orlova, J.D. Goddard, Chem. Phys. Lett. **363**, 486 (2002)
20. A. Görling, Phys. Rev. A **47**, 2783 (1993); J.P. Perdew, A. Savin, K. Burke, Phys. Rev. A **51**, 4531 (1995)
21. E. Räsänen, H. Saarikoski, M.J. Puska, R.M. Nieminen, Phys. Rev. B **67**, 035326 (2003)
22. B. Weiner, S.B. Trickey, Int. J. Quantum Chem. **69**, 451 (1998)
23. J. Paldus, G. Thiamová, J. Math. Chem. (in press)
24. R.G. Parr, *The Quantum Theory of Molecular Electronic Structure* (Benjamin, New York, 1963)
25. J. Paldus, in *Theoretical Chemistry: Advances and Perspectives*, edited by H. Eyring, D.J. Henderson (Academic, New York, 1975), Vol. 2, pp. 131–290
26. J. Paldus, J. Čížek, J. Chem. Phys. **54**, 2293 (1971)
27. M. Mataga, K. Nishimoto, Z. Phys. Chem. (Frankfurt) **13**, 140 (1957)
28. J. Paldus, E. Chin, Int. J. Quantum Chem. **24**, 373 (1983)